Repeated acoustic stimuli induce decentralized transcriptional memory for robust priming of plant defense.

Khaoula Hadj-Amor[1,2,3],Ophélie Léger[2,3¶], Sylvain Raffaele[2¶], Magdalena Kovacic[1,3], Aroune Duclos[3,4], Pedro Carvalho-Silva[2], Frédérick Garcia[1,3,&*], Adelin Barbacci [2,3,&*]

1 Université de Toulouse, INRAE, Mathematiques et Informatique Appliquées de Toulouse (MIAT), 31326 Castanet-Tolosan, France.

2 Université de Toulouse, INRAE, CNRS, Laboratoire des Interactions Plantes Micro-organismes Environnement (LIPME), 31326 Castanet-Tolosan, France.

3 Interdisciplinary research group on the effect of mechanical VIbrations on Plants (VIP).

4 Laboratoire d'Acoustique de l'Université du Mans (LAUM), UMR 6613, Institut d'Acoustique - Graduate School (IA-GS), CNRS, Le Mans Université, Le Mans, France.

* corresponding authors

E-mail: frederick.garcia@inrae.fr, adelin.barbacci@inrae.fr

¶ These authors contributed equally to this work

& These authors also contributed equally to this work

Abstract

Background

Priming plant immunity offers a powerful and sustainable strategy for crop protection, enabling plants to respond faster and more efficiently to threats. This increased readiness is driven by transcriptional memory—molecular mechanisms that store and recall stress responses, including protein accumulation, transcription factor activity, and epigenetic modifications. However, the interplay among transcriptional stress memory, its stability, and its broader impact on plant resistance remain poorly understood.

Results

Here, we reveal a tight link between transcriptional memory and defense priming in *Arabidopsis thaliana* exposed to repeated acoustic stimulations. Using a combination of experiments and computational modeling, we show that enhanced resistance to *Sclerotinia sclerotiorum* after three stimulations arises from three key mechanisms: (1) preemptive activation of defense pathways in noninoculated plants, (2) increased diversification of defense-related genes, and (3) gene priming. This heightened defense state is sustained by transcriptional stress memory across thousands of genes, which is likely orchestrated by transcription factor cascades.

Challenging the conventional view that priming involves stepwise activation of distinct pathways, our findings suggest that priming instead results from the simultaneous modulation of a broad spectrum of defense pathways. This built-in redundancy enhances resilience, shielding primed plants from the genetic variability-driven resistance loss observed in naïve plants. However, this same redundancy imposes strict limits on further enhancing the resistance. More frequent acoustic stimulations did not amplify the protective effect, and transcriptional memory faded within 1.5 days after stimulation ceased.

Conclusions

By integrating experimental and computational approaches, we present a genome-scale quantitative model of stress-induced gene regulation. Our results highlight the trade-offs inherent in transcriptional memory-driven priming, revealing both its potential and its limitations in optimizing plant immunity.

Keywords: plant resistance, quantitative disease resistance, transcriptional memory, priming, acoustic stimulations

Introduction

Plants have evolved a complex immune system to restrict or halt the progression of pathogens. Plant immunity is commonly described as an interconnected layered system (Delplace et al., 2020; Remick et al., 2023; Roux et al., 2014). The perception of conserved pathogen-associated molecular patterns (PAMPs) involves surface Pattern Recognition Receptors. PAMPs initiate a signaling cascade known as PAMP-Triggered Immunity (PTI). Pathogens have evolved effectors that can inhibit PTI but can also activate another layer of the immune system, known as Effector Triggered Immunity (ETI), upon recognition by intracellular molecular receptors. ETI triggers a rapid programmed cell death response, which is particularly effective against biotrophic pathogens that require live host cells to proliferate. ETI operates on a molecular key-lock model that, when triggered, typically confers complete immunity to the plant. However, minor variations in the structure of recognized effectors can enable the pathogen to circumvent the host perception system (Derbyshire and Raffaele, 2023a; Raffaele et al., 2010; Remick et al., 2023). In addition, pathogens that thrive on dead plant cells (necrotrophs) may use programmed cell death to their benefit (Barbacci et al., 2020; Derbyshire and Raffaele, 2023b; Govrin and Levine, 2000).

In the absence of such complete immunity, a form of disease resistance known as quantitative disease resistance (QDR) is observed, which mitigates rather than halts disease progression (Poland et al., 2009; Wang et al., 2019). QDR frequently occurs in response to necrotrophic fungi such as *Botrytis cinerea* or *Sclerotinia sclerotiorum*. The QDR is highly multigenic and involves the modulation of thousands of genes. Transcriptomic analysis of six species in the Pentapetalae botanic family revealed that approximately 30% of plant transcriptomes respond locally to infection by the necrotrophic fungus *S. sclerotiorum* (Sucher et al., 2020). Consequently, genes associated with the QDR tend to be pleiotropic and not specific to the plant immune response. In agreement with these findings, polymorphisms in the *Arabidopsis thaliana ARPC4* regulatory region, a gene that mediates actin filament reorganization, lead to increased resistance to *S. sclerotiorum* (Badet et al., 2019). The highly multigenic nature of the QDR makes it prone to influence by abiotic stresses from the environment, such as temperature variations (Aoun et al., 2017; Didelon et al., 2020; Singh et al., 2023), and internal cues, such as mechanical fluctuations in cell walls (Engelsdorf et al., 2018) indirectly induced by necrotrophic fungi (Léger et al., 2022).

Plants exposed to recurring stresses may exhibit an enhanced response after the first exposure. Plants can be conditioned to respond to a specific severe stress by initially subjecting them to a milder form of the same stress (Baier et al., 2019; Wang et al., 2014). For example, plant defense mechanisms can be activated by exposing plants to avirulent pathogens, conferring protection against secondary infections (Verhagen et al., 2010). This phenomenon in which a stress response is exacerbated by prior exposure, is often referred to as “priming” (Conrath, 2011; Liu et al., 2022). Stress exposure may also impart tolerance to unrelated stresses, as observed in wheat plants exposed to mild drought conditions, demonstrating increased resistance to low temperatures (Ru et al., 2024). This is typically designated as “cross-priming” and may rely on the potentiation of responses distinct from those to the initial stress. Priming depends on the plant's ability to memorize stress through mechanisms that are incompletely understood (Bruce et al., 2007; Crisp et al., 2016).Through alterations in plant morphology, physiology, and transcriptomic and epigenetic regulation, priming can enhance the adaptation of plants to their environment by accelerating and optimizing stress responses. In the face of challenges in agriculture due to global warming, the imperative to reduce pesticide use and the need to increase or sustain yields and harness plant priming mechanisms to design ideotypes present promising avenues for sustainable crop health management (Liu et al., 2022).

The robustness of priming phenomena in fluctuating environments is largely dependent on the dynamics and breadth of the underlying stress memory molecular mechanisms. Memory is a dynamic process by which a system acquires, stores, and retrieves information, thereby influencing its subsequent behavior. In plants, memory can take a myriad of forms characterized by distinct typical durations (Thellier et al., 2018). On a temporal scale of hours, rudimentary memory mechanisms, exemplified by the homogalacturonan cycle linked to pressure fluctuations, appear to operate autonomously of genetic influences (Barbacci et al., 2013; Proseus and Boyer, 2006). For temporal spans ranging from hours to generations, transcriptional memory involving transcription factors and epigenetic modifications has emerged as a prominent stress memory mechanism (Avramova, 2019). For example, the trimethylation of histone H3 at lysines 4 and 9 (H3K4, H3K9) is a major epigenetic modification associated with the acclimation of poplar trees to recurrent mechanical stimuli. A single bending event is sufficient to induce significant alterations in the overall abundance of this epigenetic marker (Ghosh et al., 2023). Transcription factors, which function as regulators of gene expression and mediators within signaling pathways, also play crucial roles in the intricate process of transcriptional memory, operating in synergy with epigenetic modifications. A paradigmatic example is FORGETTER3/HEAT SHOCK TRANSCRIPTION FACTOR A3 (FGT3/HSFA3), which is required for the establishment of physiological heat stress memory and the maintenance of increased expression of memory-related genes in the days following heat exposure (Friedrich et al., 2021).

Beyond these documented mechanisms, a system-level understanding of stress memory in plants is needed to evaluate the sensitivity of the underlying molecular changes to the diversity of environmental fluctuations and genetic changes. Recent studies have provided evidence that sound vibrations induce molecular and physiological changes capable of enhancing plant resistance to disease (Choi et al., 2017; Ghosh et al., 2017, 2016). Sound, characterized by minute temporal fluctuations in pressure, represents a form of mechanical stimulation. Nevertheless, the associated physical parameters complicate the elucidation of sound perception by plants. For example, a sound at 100 dB corresponds to a pressure variation of 2 Pa, constituting a minor fraction of the atmospheric pressure, and no mechanosensitive channel has been identified to respond to such low pressures (Peyronnet et al., 2014), particularly at audible frequencies exceeding a few tens of hertz (Bhandawat and Jayaswall, 2022). While the precise mechanisms underlying sound perception in plants remain elusive, numerous effects on plant biology have been documented (Appel and Cocroft, 2023, 2014; Demey et al., 2023; Hassanien et al., 2014). Concerning defense, brief exposure of *Arabidopsis thaliana* plants to fixed-intensity sound vibrations modulates genes involved in defense response and signal transduction pathways. The genes altered depend on the frequency of the sound wave, but many genes involved in disease resistance, such as AtHSPRO2 (At2g40000), AtJAZ7 (At2g34600), and At5g66070, are altered by multiple frequencies. Notably, phenotypic gains in disease resistance are reported only after repeated sound stimulation (RAS), with *A. thaliana* becoming more resistant to *B. cinerea* after 10 days of sound treatment (Ghosh et al., 2017). Transcriptomic and proteomic analyses revealed a profound effect of RAS on reprogramming the primary metabolism of plants. However, the molecular mechanisms through which RAS enables plants to transition from a susceptible state to a more resistant state remain unknown.

To gain insights into the architecture and dynamics of transcriptional stress memory underlying the emergent properties of priming, such as robustness, we studied RAS-induced disease resistance against *S. sclerotiorum* in *A. thaliana*. Our findings indicate that at least three RASs are necessary to achieve a 26% gain in resistance, independent of trichome density, which is putatively involved in sound perception. Transcriptomic analysis revealed that resistance gain was correlated with the activation of primary defensive mechanisms in noninoculated plants, including increased defense-associated gene diversification and gene priming. An in-depth investigation into transcriptional stress memory-enhancing plant defenses led to the development of a genome-scale quantitative model of the dynamics of gene regulation. Model analysis suggested that priming results from the parallel modulation of a broad spectrum of pathways rather than the sequential activation of pathways. In silico and experimental validation further confirmed that the RAS-mediated plant priming mechanism was highly resilient, operating independently of limited genetic variations associated with resistance loss in naïve plants. The robustness of priming, arising from the redundancy of gene regulatory mechanisms, also defines the limits of resistance enhancement in primed plants. In agreement with the model predictions, decreasing the interval between acoustic stimulations did not yield a corresponding increase in resistance. The predominance of gene regulation over modulation by the direct impact of acoustic stimuli resulted in a transcriptional memory persisting for only 1 day following cessation of stimuli.

Results

Transcriptional memory of AS drives the parallel activation of multiple defense pathways in the absence of pathogens.

To document the molecular changes induced by the repetition of AS, we analyzed the global gene expression of 4 week-old *A. thaliana* Col-0 plants exposed to AS corresponding to 3 hours of 1000 Hz sinusoidal waves at 100 dB (~2 Pa) once a day for 1, 3 or 8 days (**Fig. 1A**). A mature leaf from each plant was collected for RNA extraction. Compared with those in plants not exposed to AS, 10% (3 RAS) to 24% (8 RAS) of *A. thaliana* genes were differentially expressed (DEGs) upon AS (**Fig. 1B, SFile 1**). Overall, 35% of the *A. thaliana* genes (9554) were DEGs under at least one RAS modality, among which 1422 (15%) were DEGs independent of the number of AS, and 5578 (58%) were modulated by a specific number of AS. These results indicate that a transcriptional memory effect (**Fig. 1D**) targets a majority of RAS DEGs and highlights the ability of plant cells to distinguish between single and repeated stresses.

To gain insight into the functional reprogramming of plants by RAS, we analyzed gene ontologies (GOs) (Ge et al., 2020) enriched among DEGs associated with 1 or more (“1+”) AS (**Fig. 1C, SFile 2**), among DEGs associated with 3 or more (“3+”) RASs and DEGs associated with only the 8th RAS. After 1 AS, the DEGs were dominated by genes associated with the response to different stresses (abiotic, osmotic stress, endogenous stimulus, response to ethylene, light, hypoxia), as well as processes associated with plant-pathogen interactions, such as the response to chitin and the response to other organisms (**Fig. 1C**). After 3 RASs, GOs were accompanied by processes associated with responses to oxoacids such as oxalic acid secreted by *Sclerotinia sclerotiorum* (Cessna et al., 2000) and the biosynthesis of carbohydrate structural elements (**Fig. 1C**). Only 3 supplementary biological processes (GO) terms were enriched in DEGs after 8 RASs. The cellular component GO terms were dominated by Golgi and cell-cell junctions upon 1 AS, complemented by the endoplasmic reticulum and cell wall upon 3 RASs, and the cytoskeleton and plastids upon 8 RASs (**Fig. 1C**). DEG analysis confirmed the involvement of mechanosensing and osmosensing in the transcriptional memory of RAS (**Fig S1**). We identified 142 MTI (Mechano-signaling Triggered Immunity)-associated genes that were differentially expressed upon RAS, only 18% (25 genes) of which were regulated independently of the number of RASs (**Fig S2, SFile 3**). We also identified 31 epigenetic regulators associated with thermomemory and defense that were differentially expressed upon RAS, 10 of which exhibited regulation specific to the number of AS (**Fig. S3, SFile 3**). Therefore, the transcriptional memory of RAS did not result from the sustained activation of mechanisms triggered after the first AS, but rather from the activation of parallel mechanisms over AS repetitions.

To gain insight into how the transcriptional reprogramming induced by RAS altered plant immune responses, we compared RAS-triggered DEGs with DEGs in plants inoculated with the necrotrophic fungus *S. sclerotiorum* (not exposed to AS). Among the 14040 DEGs identified upon fungal pathogen inoculation, 7108 (51%) were also DEGs upon RAS in the absence of the pathogen (**Fig. 1E**). A total of 14% of the DEGs in 3 RASs (2635 genes) were also differentially expressed upon pathogen inoculation, and 33% of the DEGs in 1 and 8 RASs (5865 and 6452 genes respectively) were differentially expressed upon pathogen inoculation. All DEGs were modulated by RAS and pathogen inoculation in the same direction, with similar proportions of up- and downregulated genes shared between RAS and pathogen-responsive genes. We conclude that a majority of genes responsive to fungal pathogen inoculation respond to RAS alone, and reciprocally, a large proportion of RAS-responsive genes are associated with the pathogen response. Together, these results show that the transcriptional memory of AS leads to the parallel regulation of multiple genetic pathways associated with the pathogen response.

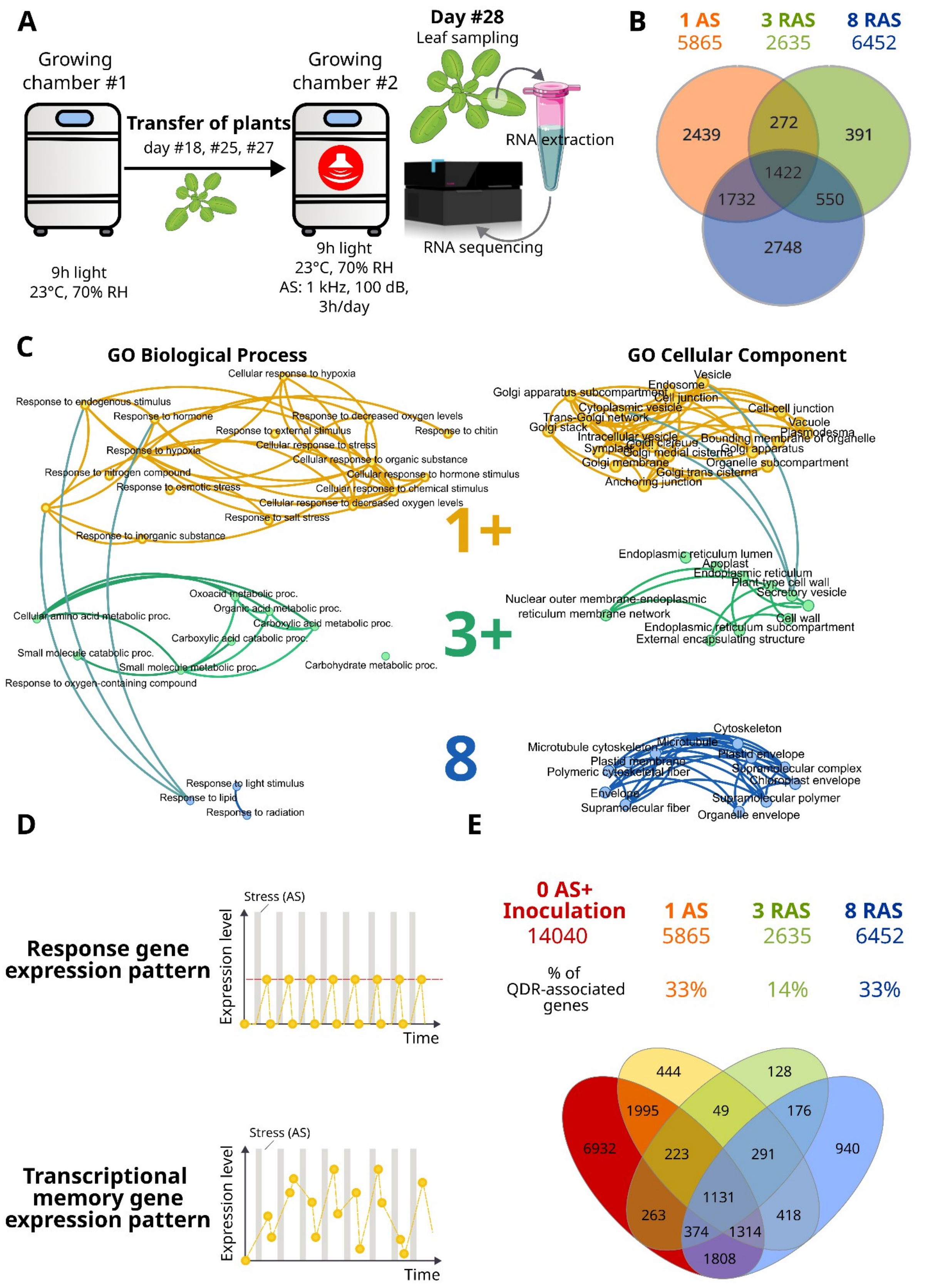
A
Growing chamber #1
9h light
23°C, 70% RH
Transfer of plants
day #18, #25, #27
Growing chamber #2
9h light
23°C, 70% RH
AS: 1 kHz, 100 dB, 3h/day
Day #28
Leaf sampling
RNA extraction
RNA sequencing
B
1 AS
5865
3 RAS
2635
8 RAS
6452
2439
272
391
1422
1732
550
2748
C
GO Biological Process
Cellular response to hypoxia
Response to endogenous stimulus
Response to hormone
Response to decreased oxygen levels
Response to external stimulus
Response to chitin
Cellular response to stress
Response to hypoxia
Cellular response to organic substance
Response to nitrogen compound
Cellular response to hormone stimulus
Response to osmotic stress
Cellular response to chemical stimulus
Cellular response to decreased oxygen levels
Response to salt stress
Response to inorganic substance
Oxoacid metabolic proc.
Organic acid metabolic proc.
Cellular amino acid metabolic proc.
Carboxylic acid metabolic proc.
Carboxylic acid catabolic proc.
Small molecule catabolic proc.
Small molecule metabolic proc.
Carbohydrate metabolic proc.
Response to oxygen-containing compound
Response to light stimulus
Response to lipid
Response to radiation
1+
3+
8
GO Cellular Component
Vesicle
Endosome
Golgi apparatus subcompartment
Cell junction
Cytoplasmic vesicle
Cell-cell junction
Trans-Golgi network
Golgi stack
Vacuole
Plasmodesma
Intracellular vesicle
Golgi cisterna
Bounding membrane of organelle
Symplast
Golgi medial cisterna
Golgi apparatus
Golgi membrane
Organelle subcompartment
Golgi trans cisterna
Anchoring junction
Endoplasmic reticulum lumen
Apoplast
Endoplasmic reticulum
Plant-type cell wall
Secretory vesicle
Nuclear outer membrane-endoplasmic reticulum membrane network
Cell wall
Endoplasmic reticulum subcompartment
External encapsulating structure
Cytoskeleton
Microtubule cytoskeleton
Microtubule
Plastid membrane
Plastid envelope
Polymeric cytoskeletal fiber
Supramolecular complex
Chloroplast envelope
Envelope
Supramolecular polymer
Supramolecular fiber
Organelle envelope
D
Response gene expression pattern
Stress (AS)
Expression level
Time
Transcriptional memory gene expression pattern
Stress (AS)
Expression level
Time
E
0 AS+ Inoculation
14040
1 AS
5865
3 RAS
2635
8 RAS
6452
% of QDR-associated genes
33%
14%
33%
444
128
1995
49
176
6932
223
291
940
1131
263
418
374
1314
1808

Figure 1. Impact of RAS on Gene Expression in non-inoculated Plants. A. Experimental protocol overview. **B.** Venn diagrams illustrating the genes expressed after 1, 3, and 8 RASs in non-inoculated plants. **C.** Enrichment analyses of biological processes and cellular component ontologies during RAS. A link between two nodes indicates that the two ontologies share more than 20% of genes. 1+ indicates the enrichments present at 1, 3, and 8 RAS; 3+ indicates the

enrichments present at 3 and 8 RAS; 8 indicates the enrichments present at 8 RAS only. **D**. Gene expression patterns associated with repeated stresses. The response genes presented consistent expression levels following each stimulation. The expression levels of transcriptional memory-associated genes are contingent upon the prior history of stimulation. **E**. Venn diagrams representing genes expressed after 1, 3, and 8 RAS in non-inoculated plants compared with those in plants not subjected to RAS but infected with *Sclerotinia sclerotiorum*. The numbers indicate the total count number of differentially expressed genes.

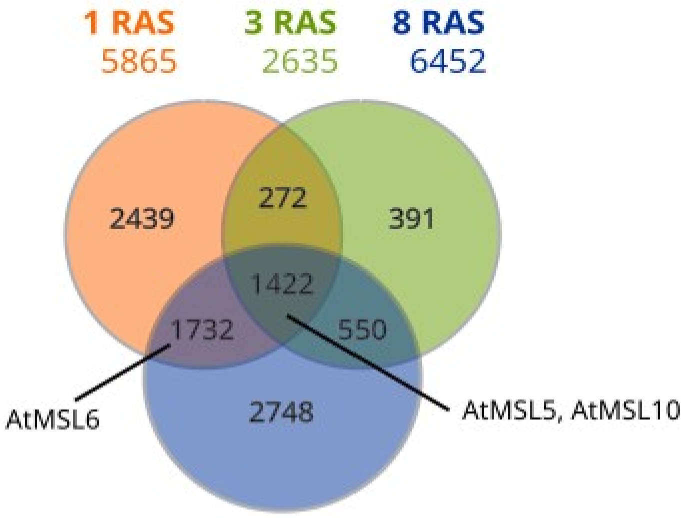

Figure S1. Mechanosensitive Like channels (MSLs) differentially expressed by RAS in non-inoculated *A.thaliana* plants.

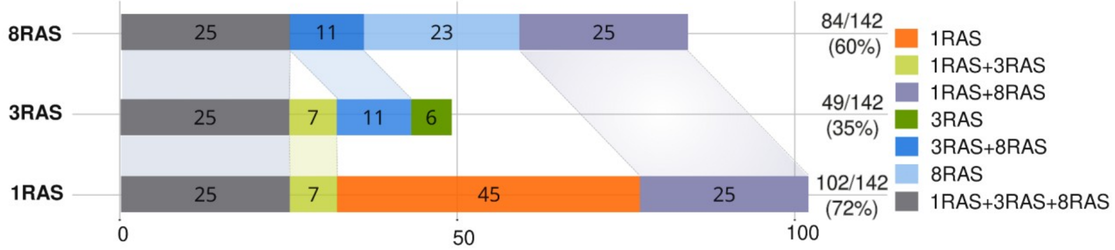

Figure S2. Transcription of genes associated with MTI (Mechanosignaling Triggered Immunity) genes over RAS.

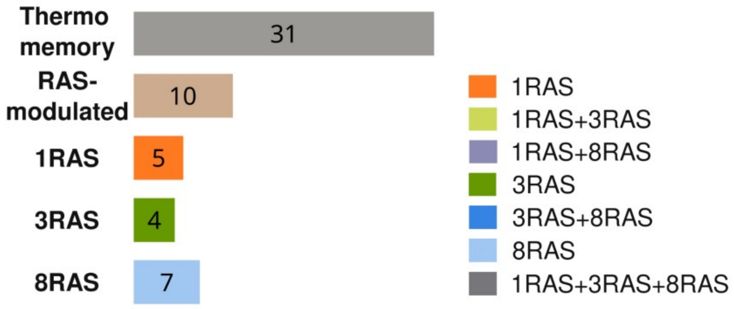

Figure S3. Epigenetic regulators associated with thermomemory and defense are differentially expressed upon RAS. Ten epigenetic regulators exhibit regulation specific to the number of AS.

A transcription factor cascade diversifies AS-mediated transcriptome reprogramming at each repeat

We hypothesized that the diversification of GO terms that were differentially regulated after each RAS could result from the sequential activation of transcription factors (TFs) with distinct target gene repertoires. To support this hypothesis, we focused on TFs differentially expressed upon RAS and their predicted target genes identified, owing to the cis-binding motifs listed in the PlantTFDB (Jin et al., 2017) (**Fig. 2, SFile 4**). TF expression was contingent upon the number of RAS exposures, with only 117 (20%) TFs being modulated independently of the AS count. Following exposure to 1 AS, 176 TFs (TFs_{1AS}) and 5 227 of their predicted targets were DEGs, representing 89% of all DEGs upon 1 AS. Among the predicted targets of TFs_{1AS}, 80 were differentially regulated by 3 RAS (TFs_{3RAS}). The predicted targets of TFs_{3RAS} included 1957 DEGs upon 3 RASs, representing 74% of the DEGs upon 3 RASs. Among the predicted targets of TFs_{3RAS}, 163 were TFs differentially regulated by 8 RASs (TFs_{8RAS}). The predicted targets of TFs_{8RAS} included 5845 DEGs upon 8 RASs (24.5 targets per TF_{3RAS} in average), representing 90% of the DEGs upon 8 RAS. Overall, the differential expression of 91% of RAS DEGs (9039 genes) could be explained by the sequential activation of 254 TFs at each AS repeat. Therefore, a cascade of TF regulation by RAS could explain the overall kinematics of transcriptional memory (**Fig. 2**). Similar to the findings of mitotic bookmarking observed in animals (Bellec et al., 2018), our findings suggest that TFs retained on their targets act as a somatic bookmarking of past states, enabling plants to discern the number of stimuli. All 18 known TFs associated with MTI pathways were implicated in the TF transcription cascade, confirming the recruitment of MTI pathways in transcriptional memory.

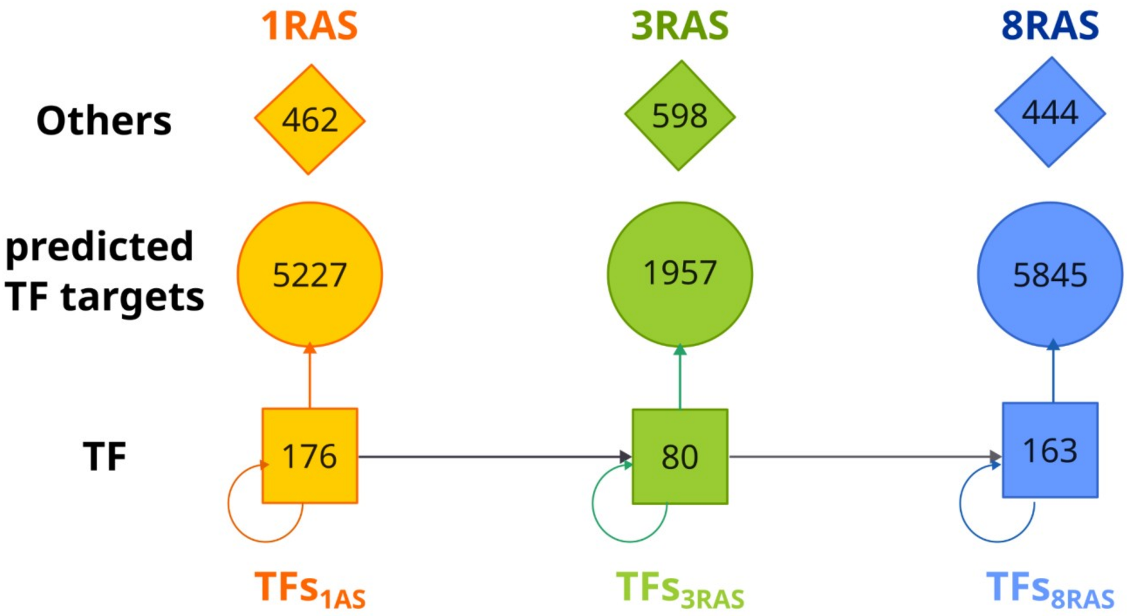

Figure 2. Transcription factor regulation cascade over RAS. The numbers in nodes indicate the counts of either transcription factors (TFs, squares) or other genes (circles) differentially expressed by RAS. The numbers over arrows indicate the number of regulations. The genes that are differentially expressed following RAS but independent of TFs are indicated by diamonds.

AS-induced disease resistance requires repeated stimulations.

To investigate the impact of RAS on plant defense, we applied AS corresponding to 1000 Hz sinusoidal waves at 100 dB for 3 hours every day for 0, 1, 2, 3, or 10 days before inoculation with *S. sclerotiorum* (**Fig. 3A, SFile 5**). Disease resistance was quantified by evaluating the growth rate of necrosis in leaves according to Barbacci et al. (2020). A single AS led to a 16% increase in disease susceptibility (Welch's test p-value 4.3E-4), whereas a minimum of 2 RASs led to an increase in disease resistance. Two RASs elicited a slight but significant 11% increase in disease resistance (Welch's test p-value 0.022). Beyond 3 RASs, a substantial ~25% gain in disease resistance was observed and remained similar in plants subjected to 10 RASs (Welch's test, p-value 3.3E-5 and 1.2E-5 at 3 and 10 RASs respectively, **Fig. 3A**). A similar gain of disease resistance after 10 RAS (Type II ANOVA, RAS: p-value = 2.79e-09, genotype: p-value = 9.98e-01, genotype x RAS: p-value = 9.54e-01) was observed for mutant plants altered in trichome morphology (*arpc4-t2* (Badet et al., 2019)) and density (*gl-1* glabrous (Benikhlef et al., 2013)), indicating that RAS defense priming was largely independent of trichomes in our assay (**Fig 3B**). Contrasted defense priming phenotypes according to the number of AS suggested that RAS-induced disease resistance was a dynamic process contingent upon the temporal integration of the plant's response to RAS.

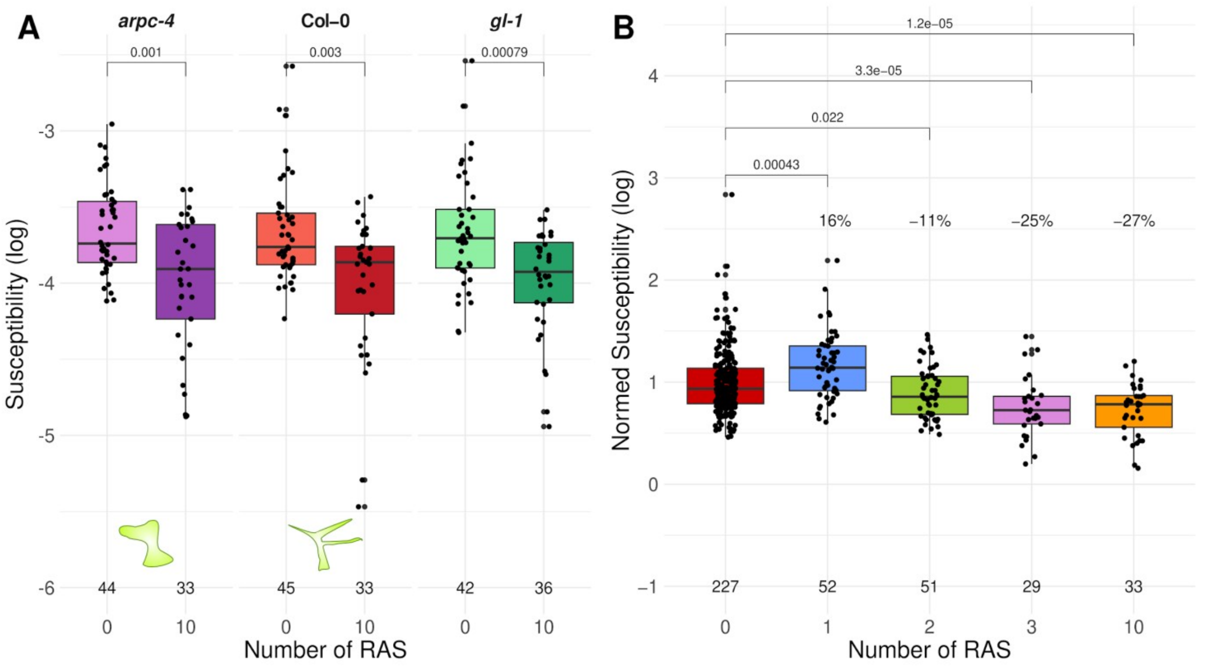

Figure 3. Impact of repeated acoustic stimulations (RAS) on plant susceptibility to *Sclerotinia sclerotiorum*. A. Approximately 25% reduction in susceptibility was observed with 3 hours of daily stimulation over 10 days, irrespective of the genotype affecting trichomes. **B.** A decrease in susceptibility induced by repeated acoustic stimulation was established after three stimuli and maintained consistently. Boxplots indicate the interquartile range from the 25th to the 75th percentile, with the bold line representing the median. To increase the granularity of the information, jittered points are overlaid on the boxplot. Unpaired Welch's test p-values are indicated in the figure. The number of samples is indicated under each boxplot.

RAS broadened and intensified the activation of QDR-associated genes to prime plant defense

To study the transcriptional changes associated with disease resistance priming by RAS, we exposed *A. thaliana* Col-0 plants to 0, 1, 3 and 8 RASs before inoculation with *S. sclerotiorum* and RNA-sequencing 24 hours post-inoculation (**Fig. 4A**). We first analyzed DEGs by comparing gene expression in RAS-exposed and subsequently infected plants with non-inoculated naïve plants (**SFile 6**). Out of 14 040 DEGs identified upon inoculation in naïve (no RAS) plants, 96% were also DEGs in plants exposed to RAS and inoculated (**Fig. 4B**), consistent with a dominant effect of the last stress in transcriptome studies of sequential stresses (Desaint et al., 2021). Second, to highlight defense genes regulated by the transcriptional memory of RAS, we compared DEGs in (i) non-inoculated RAS-treated plants, (ii) plants inoculated following RAS treatment and (iii) inoculated plants not treated with RAS (**Fig. 4C**). Genes differentially expressed only following the sequence of RAS treatment and pathogen inoculation were 1873 after 1 AS, 1 364 after 3 RASs and 1 736 after 8 RASs. These genes represented QDR genes with a transcriptional memory-dependent expression (QDR_{TMD}). Overall, we identified 2 987 QDR_{TMD} genes, representing a 21.2% expansion to 14 040 DEGs upon inoculation in naïve (no RAS) plants. Among the QDR_{TMD} genes, only 584 (19.5%) were modulated regardless of the number of AS (**Fig. 4D**).

To obtain an overview of the nature of QDR_{TMD} genes, we performed GO enrichment analyses by comparing QDR_{TMD} genes with genes differentially expressed in plants not exposed to AS (**Fig. 4E, SFile 7**). The biological processes enriched among the QDR_{TMD} genes varied with the number of RASs and were dominated by processes associated with defense responses (**Fig. 4E**). After 3 RAS, QDR_{TMD} genes were enriched in genes associated with defense responses to fungi and bacteria. For 8 RAS, no additional enrichment was observed despite the greater number of differentially expressed genes compared to after 3 RASs. For 8 RASs, no additional enrichment was observed despite the higher number of differentially expressed genes compared to after 3 RASs. Nevertheless, in the context of pathogen inoculation, past RASs led to the diversification of QDR pathways activated in inoculated plants.

A defining feature of primed genes is a faster and stronger response following exposure to successive stresses (Ghosh et al., 2021). To assess the extent to which RAS-induced transcriptional memory drives gene priming, we identified genes exhibiting a greater log-fold change in expression upon pathogen inoculation in RAS-treated plants compared to naïve plants. We identified 12 732 RAS-primed genes following 3 and 8 RASs in comparison with naïve plants and plants exposed to 1 AS (**Fig. 4F**). These included 351 QDR$_{\text{TMD}}$ genes and140 MTI-associated genes. GO enrichment analysis revealed greater enrichment (FDR 6.1e-3) of QDR$_{\text{TMD}}$ primed genes in the defense response to bacteria GO compared to other QDR$_{\text{TMD}}$ genes. Together, these results show that RAS-triggered transcriptional memory leads to an increased defense response through the diversification of the transcriptional response to pathogen inoculation and the priming (induction of faster and stronger responses) of plant QDR genes.

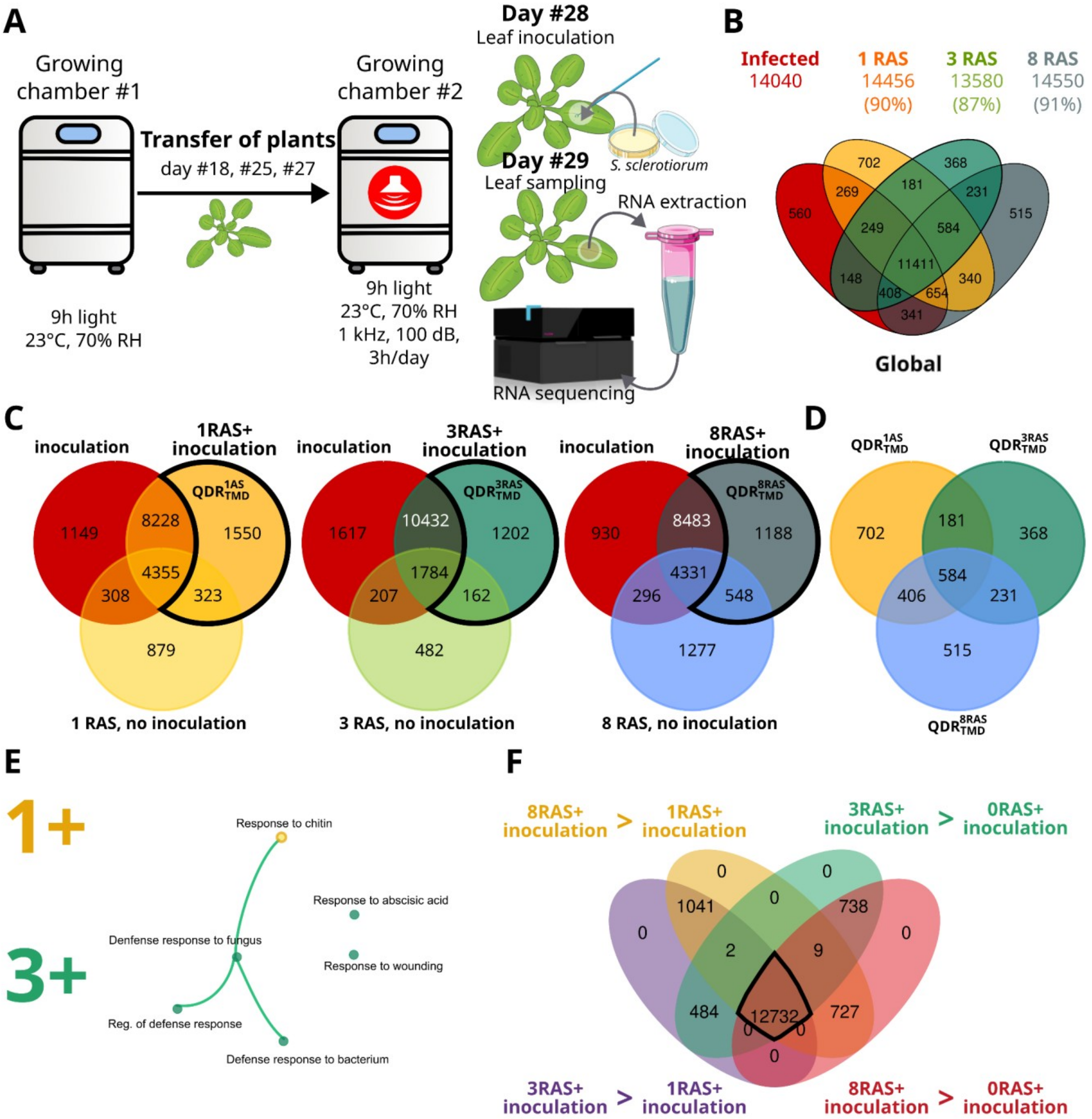
A
Growing chamber #1
Transfer of plants
day #18, #25, #27
9h light
23°C, 70% RH
Growing chamber #2
9h light
23°C, 70% RH
1 kHz, 100 dB,
3h/day
Day #28
Leaf inoculation
S. sclerotiorum
Day #29
Leaf sampling
RNA extraction
RNA sequencing
B
Infected
14040
1 RAS
14456
(90%)
3 RAS
13580
(87%)
8 RAS
14550
(91%)
560
702
269
181
368
231
515
249
584
11411
148
408
654
340
341
Global
C
inoculation
1RAS+ inoculation
QDR1AS TMD
1149
8228
1550
4355
308
323
879
1 RAS, no inoculation
inoculation
3RAS+ inoculation
QDR3RAS TMD
1617
10432
1202
1784
207
162
482
3 RAS, no inoculation
inoculation
8RAS+ inoculation
QDR8RAS TMD
930
8483
1188
4331
296
548
1277
8 RAS, no inoculation
D
QDR1AS TMD
QDR3RAS TMD
702
181
368
584
406
231
515
QDR8RAS TMD
E
1+
3+
Response to chitin
Response to abscisic acid
Denfense response to fungus
Response to wounding
Reg. of defense response
Defense response to bacterium
F
8RAS+ inoculation > 1RAS+ inoculation
3RAS+ inoculation > 0RAS+ inoculation
0
0
1041
0
738
0
0
2
9
484
12732
727
0
0
0
3RAS+ inoculation > 1RAS+ inoculation
8RAS+ inoculation > 0RAS+ inoculation

Figure 4. Impact of RAS on Gene Expression in Plants Exposed to RAS and inoculated. A. Experimental protocol overview **B**. Venn diagrams illustrating genes expressed after 1, 3, and 8 RASs in infected plants compared with the transcriptome of naïve inoculated plants. **C**. Venn diagrams showing genes expressed during infection after RAS in non-inoculated and inoculated plants. **D**. Venn diagram highlighting $\mathrm{QDR_{TMD}}$ genes expressed in RAS-exposed plants before infection modulated in the context of infection. **E**. Enrichment analyses of biological process ontologies in $\mathrm{QDR_{TMD}}$ genes. A link between two nodes indicates that the two ontologies share more than 20% of genes. **F.** Venn diagram showing genes primed by 3 or 8 AS in inoculated plants. $\mathrm{QDR_{TMD}}$, quantitative disease resistance genes with transcriptional memory-dependent expression; RAS, repeated acoustic stimulation.

Dynamic modeling reveals the decentralized nature of RAS transcriptional memory

To gain a better understanding of the genetic basis of the dynamics of RAS-induced transcriptional memory, we constructed a dynamic genome-scale network for non-inoculated plants exposed to RAS. Given the considerable number of genes and the limited temporal resolution, we followed the standard approach of clustering similarly shaped trajectories. We employed a robust clustering approach based on the sign of expression variation following each AS. This method is suitable for very short time series categorized genes into positive (+), negative (-), or null (=) variation between consecutive AS. Among the resulting 26 clusters (**Fig. 5A**), five had less than 5 genes (clusters 1, 2, 5, 14 and 23) and the largest (cluster 18) included 2 294 genes (**Fig. 5A**). Overall, the number of RAS-primed genes was proportional to the number of genes in each cluster. We identified biological process GO enrichments in 15 clusters, reflecting the diversity of processes regulated by RAS (**Fig. 5A**), including defense-related processes (clusters 10, 12, 16 and 21), protein biosynthesis (clusters 20, 24), metabolism (clusters 4, 6, 7, 8 and 13), the regulation of transcription and cell trafficking (clusters 9, 11). GOs reflected structural alterations such as cell wall organization (cluster 6) and microtubule-dependent movements (clusters 4, 22), which are fundamental to MTI and plant defense. Several small clusters with no GO enrichment harbored genes associated with response to cold stress (cluster 1, 3, 15), drought (cluster 14, cluster 19), and defense (cluster 17). The 142 MTI-associated genes distributed into 14 clusters, the 469 TFs distributed into 19 clusters, and the 12732 RAS-primed genes distributed proportionally to the cluster's size, highlighting the decentralized nature of sound perception.

To capture gene interactions, we employed a network modeling approach. Assuming time-independent molecular regulations, we formulated gene expression dynamics as $\Delta X_N = (X_{N+1}-X_N) =$

$A.X_N + AS_{Systematic\ effect}$, where ΔX_{RAS} represents the variation in the vector of the representative expression level of a gene clusters between the Nth and the N+1th AS, X denotes the vector of representative expression level of gene clusters, A is a time-independent regulation matrix describing the dynamic regulation of all other gene clusters, and the $AS_{Systematic\ effect}$ is a vector of fixed effects characterizing constant RAS impacts on gene expressions. The resulting dynamic network consisted of the 26 clusters with average number of neighbors of 12.31, interconnected by 184 oriented edges with characteristic path length 2.3 (**Fig. 5B**). All but four clusters (12, 20, 23 and 24) had both incoming and outcgoing links, unveiling a highly-connected non-hierarchical network organization (**Fig. 5B**). Cluster 23, formed by the single *CSS* gene (copper chaperone for SOD1, AT1G12520) had no incoming link and connected outward to cluster 3 only. The three terminal nodes (no outward link) of the network consisted of clusters 12, 20, and 24 containing 665 genes in total, with functions related to response to stress and protein biosynthesis and including 20 MTI genes, 49 TFs, and 519 RAS-primed genes. The nodes with the highest betweenness centrality consisted of clusters 10, 3, and 11, containing 124 genes in total, including the major defense TFs WRKY33, NAC019, and NAC062, the stress-response genes KIN1 and COR15a, and the defense-related genes PR4, PSK4, and HIR1.

To emphasize the dynamic implementation of transcriptional stress memory over RASs, for each cluster, we calcultaed the relative variation in gene expression between consecutive RASs as $(X_1-X_0)/X_0$, $(X_3-X_1)/X_1$, $(X_8-X_3)/X_3$ (**Fig. 5C**). Clusters 13, 11, and 12 were most affected by one AS, while clusters 22, 4, and 2 were most impacted after 3 RAS. For 8 RAS, the most affected clusters were 2, 22, 11, and 25. 18 clusters (69%, **Fig. 5A**) showed an $AS_{Systematic\ effect}$, indicating that the transcriptional memory of AS drives broad gene expression reprogramming rather than the activation of specific transduction cascades. Cluster 4, associated with microtubule activity, showed a strong dependence on the $AS_{systematic\ effect}$ (-1.4), reinforcing the central role of this activity in RAS perception. These modeling results suggest that the activation of RAS-associated transcriptional memory extends well beyond the classical mechano-responsive genes, encompassing genes with diverse functions and diverse RAS response patterns. This non-hierarchical and intricate organization facilitates the diversification of defense priming in plants exposed to RAS and could provide a basis for a robust and adaptive priming response at the cellular level.

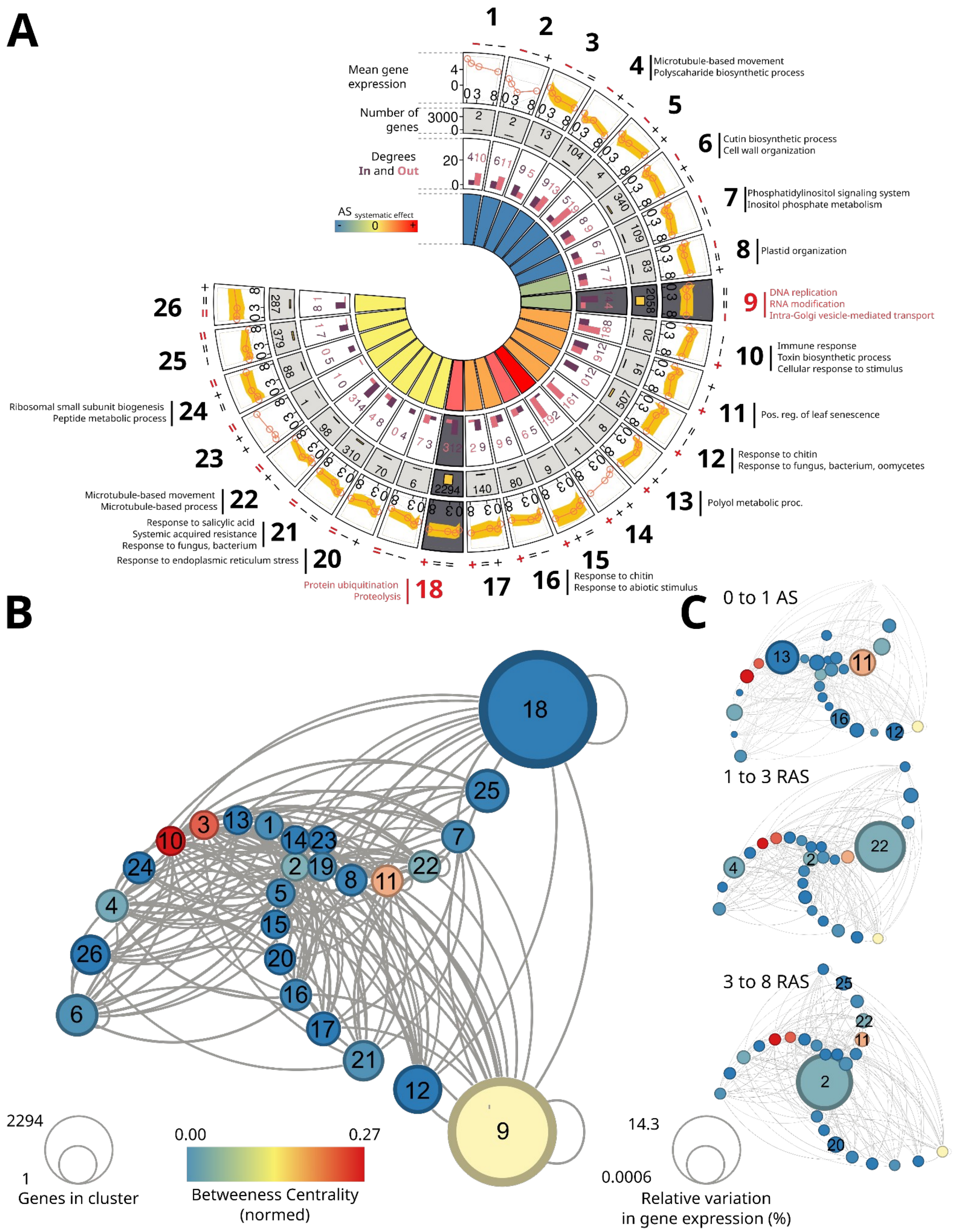

Figure 5. Dynamic Model of Plant Priming through Repeated Acoustic Stimulations (RAS). A. Characteristics of g clusters, their network connections, and the RAS-induced effect (B in the model) on gene expression. **B.** Dynamic model of gene regulation (A matrix in the model) organized into four communities. **C.** Relative variations in gene expression during RAS.

Defense priming by RAS is robust to genetic perturbations and increased stimulation frequency.

To test the extent to which the topology of the RAS network underpinned robust plant defense, we performed a systematic in-silico coarse knockout analysis by altering the weight of regulatory connections established by each gene cluster by +1%. We hypothesized here, that the knockout of a gene results in a variation in the regulations of the cluster to which this gene belongs. This hypothesis is quite strong and is only reasonable if the genes knocked out in-silico do not impact the entire network, as would be the case, for instance, with genes involved in hormonal pathways such as JA, SA, or ethylene. We then calculated the consecutive variation in the Root Mean Square Error (RMSE) induced in other clusters after 3AS (**Fig. 6A**). In-silico mutations lead to RMSE variations between 0.0 and 1.86% for the 24 clusters with more than one gene, in the same range as the introduced variation. This finding indicated that the alteration of gene regulation is not amplified in this network, suggesting that plant defense priming by RAS results from the synergistic response of all gene clusters and is generally robust to local genetic alterations. To corroborate this prediction experimentally, we monitored the variation in the resistance phenotypes of primed and naïve plants altered in mechanoperception pathways that were differentially expressed upon *S. sclerotiorum* infection. For this purpose, we exposed the MSL quintuple mutant (msl4-5-6-9-10, denoted Δ5) and the mca1 mutant lines to 3 RASs before inoculation with *S. sclerotiorum* (Tran et al., 2021; Yamanaka et al., 2010). The naïve mutant plants were more susceptible than naïve wild-type plants (p-value 0.01 and 2.4E-10 for Δ5 and mca1 respectively), supporting a role for the associated pathways in the control of plant defense (**Fig. 6B**). However, mutant plants exposed to RAS before inoculation showed a strong defense priming effect (p-value 3.6E-12 and 6.6E-10 for mca1 and Δ5 respectively), making them as resistant as primed wild type plants (not significant).

To assess the effect of AS frequency on plant defense priming, we used our dynamic model to simulate the average gene expression in each cluster after 8 days of RAS for varying numbers of RASs per day (1 AS every 3 days to 3 RASs per day, **Fig. 6C**). An increase in the number of acoustic stimulations per day had minimal effects on representative cluster gene expression. However, when the stimulations were spaced more than 1 day apart, a majority of the clusters presented significant deviations in their expression profiles (notably clusters 4, 6, 7, 10, 11, 12, 16, 17, 18, 20, 21, 22, 25). To challenge the model's prediction regarding the minimal impact of an increased number of daily stimulations, we exposed *A thaliana* Col-0 plants to two RASs of 3 hours per day for 3 days before inoculation with *S. sclerotiorum*. Compared with naïve plants, plants exposed to two RASs per day remained less sensitive but slightly more susceptible than those exposed to only one AS per day (**Fig. 6D**).

These results demonstrate that priming by RAS restored the resistance phenotype of plants impaired in mechanoperceptive pathways. As suggested by the model, plant priming by RAS may involve intricate pathways that act synergistically. The high degree of interconnection between pathways contributes to robust priming mechanisms that are less dependent on genetic variation and increased AS frequency.

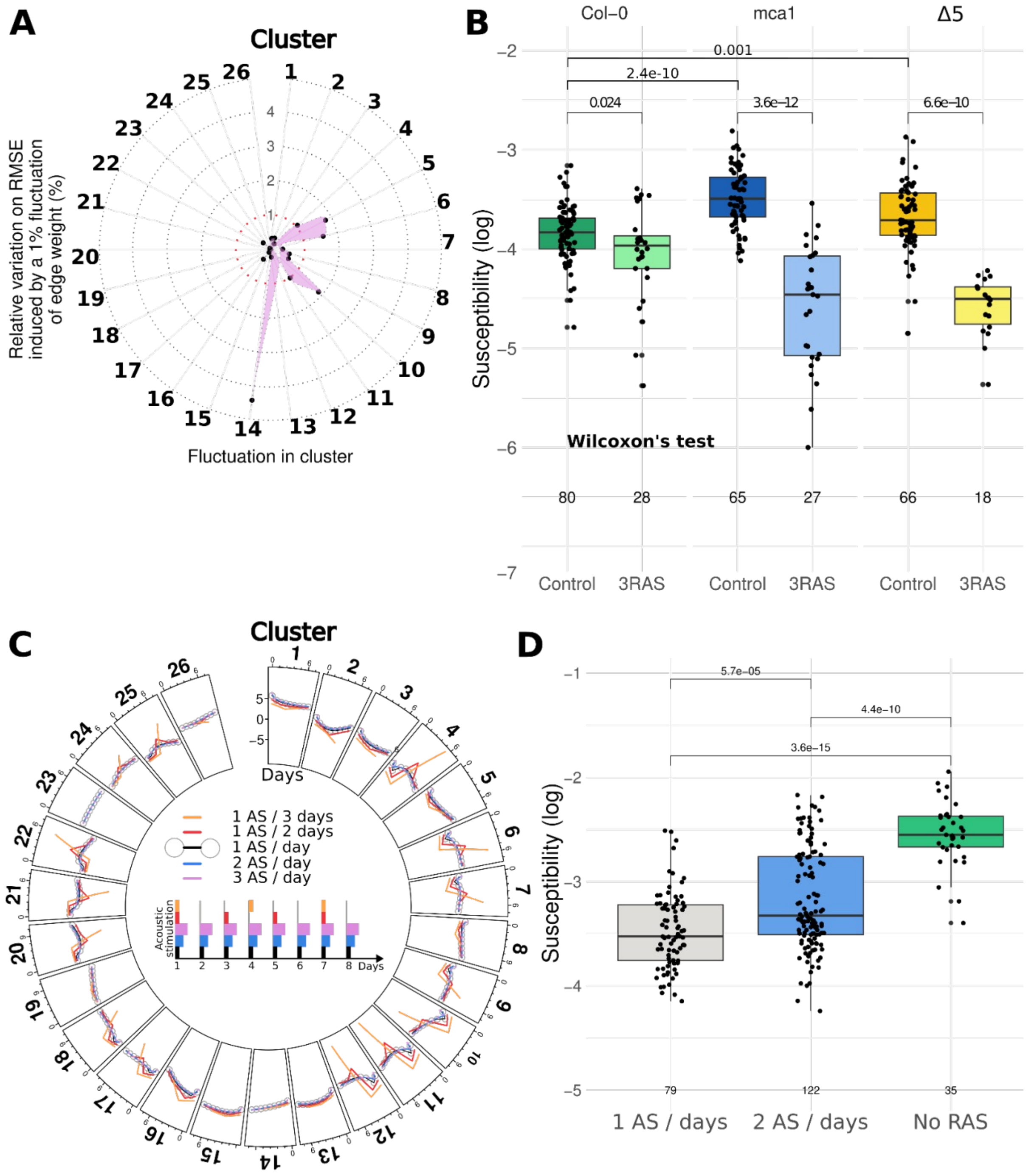

Figure 6. Robustness of the priming of plant defense by RAS. A. Simulation depicting the relative variation in Root Mean Square Error (RMSE) of gene expression caused by a +1% fluctuation in gene regulation by each cluster. **B.** Phenotypic variation in susceptibility between naïve plants and plants exposed to Acoustic Stimulation (AS) three days before infection, as illustrated for three different genotypes. **C.** Variations in gene expression associated with more and less frequent AS. Variation depicted over 8 days (external layer) with a description of the stimulation pattern (inner layer). **D.** Phenotypic variations in the susceptibility for plants exposed to different RAS frequencies to *S. sclerotiorum*.

Defense priming due to the transcriptional memory of RAS is short-lived

Our dynamic model suggested that RAS sparser than once per day leads to significant deviations in the expression of genes from many clusters, questioning the persistence of the transcriptional memory of RAS. The inquiry into the length of transcriptional memory arose from disruptions in gene expression following infrequent stimulation. To delve deeper into the temporal aspects of memory, we analyzed the eigenmodes of the regulation matrix A. Each mode represents a linear combination of clusters, describing how the average gene expression within clusters varies in the absence of AS. These eigenmodes were derived by computing the eigenvectors of matrix A, revealing that out of the 26 modes analyzed, 14 were stable, characterized by eigenvalues with negative real parts, including 7 oscillatory ones (with a nonzero imaginary part) whose period was proportional to their imaginary component. (**Fig. 7A**). The remaining 12 unstable eigenmodes (6 oscillatory ones) had a limited contribution to total gene expression, indicating a weak effect on gene expression over the 8-day period of interest (**Fig. 7A**). We then observed that among the 14 stable modes, only 6 had a reset time of less than 8 days. Additionally, the periods of the oscillatory modes were all well beyond 8 days, indicating low reactivity on a timescale of a few days (**Fig. 7B**). The 6 eigenmodes with reset times ranging from 1.47 to 6.8 days, embodied variations in 25 out of 26 clusters. Eigenvalue analysis, therefore, estimated that the overall reset time of plant memory was close to 1.5 days, suggesting that a primed plant exposed to 3 RASs would lose transcriptional memory of priming after 1.5 days without AS. To validate experimentally the predicted duration of the memory window, Col-0 plants were subjected to 3 RASs and inoculated with *S. sclerotiorum* 0, 1, 2, and 3 days after the last stimulation. naïve plants (no AS) were inoculated at the same time to serve as controls (**Fig. 7C**). Inoculation immediately after 3 RASs led to a 25% decrease in susceptibility compared to naïve plants (**Fig. 3B**). When 3 RASs were followed by a delay of one day before pathogen inoculation, we observed a 14% decrease in susceptibility (p-val. 6.2E-03, **Fig. 7C**). The decrease in susceptibility after 3 RAS vanished with 2-day or longer delay between 3 RAS and pathogen inoculation (p-val 0.23, 2 days, p-val 0.99 3 days, **Fig. 7C**). Therefore, in the line with model predictions, the defense priming effect of RAS vanished between 1 and 2 days without AS prior pathogen inoculation. We conclude that defense priming due to the transcriptional memory of the RAS is relatively short-lived, and is largely lost after two days without AS, emphasizing the need for repeated stimulation to yield a robust and adaptive cellular response to sound.

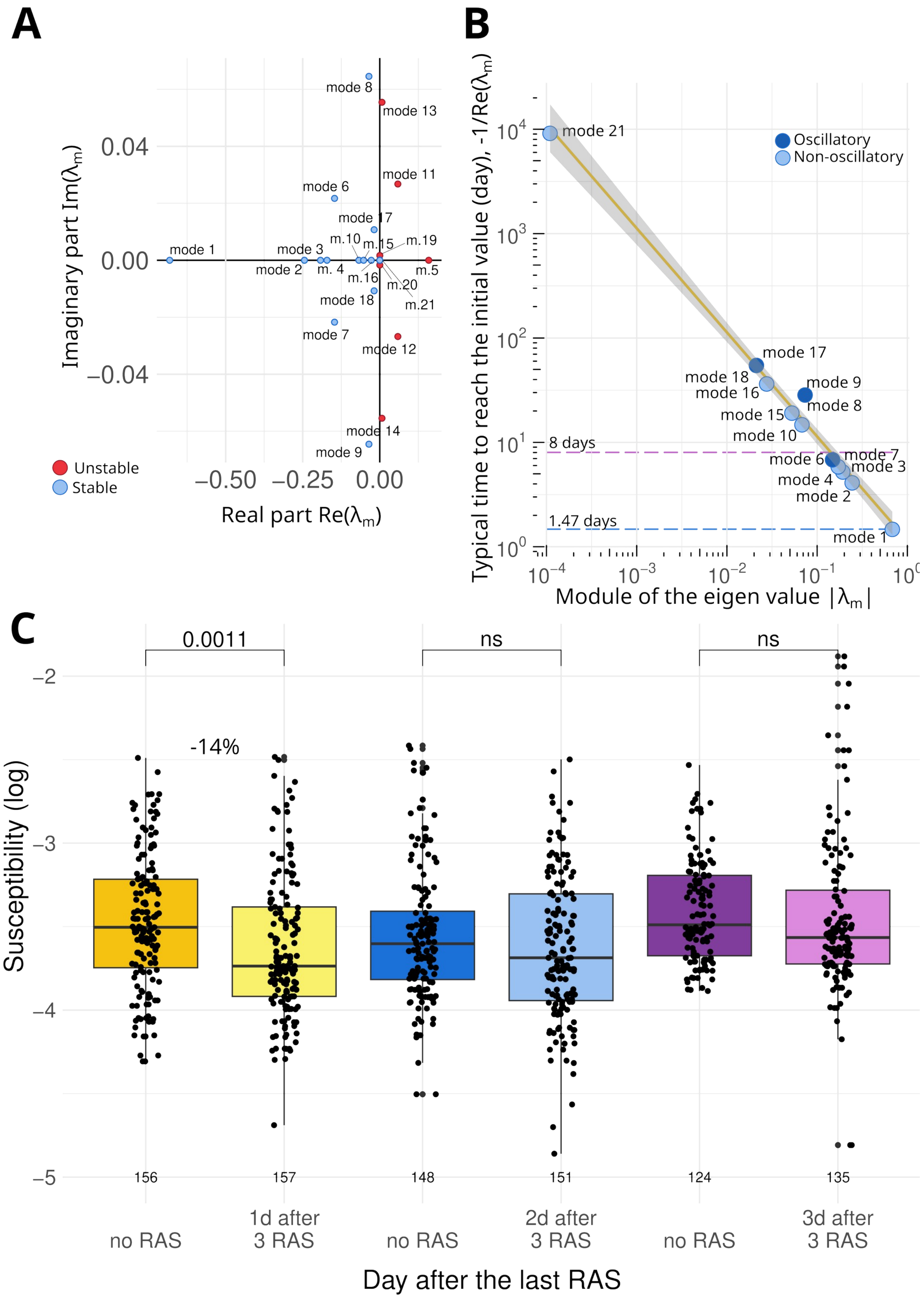

Figure 7. Memory reset time. A. The modes and their eigenvalues. Modes with a negative real part are stable. Modes with a nonzero imaginary part are oscillatory. The stable modes are in blue, and the unstable modes are in red. **B.** Relation between the typical time required for a mode to reach its initial value (reset time) and its

module. **C.** Phenotypic variations of *A. thaliana* plants exposed to 3 RASs and infected 1, 2, and 3 days after the last AS.

Discussion

Transcriptional stress memory is closely linked to the priming of plant resistance. The transition of plants from a naïve state to a primed state, in which they respond more rapidly and effectively to environmental stresses, is a dynamic process that remains largely unknown and poorly described. In this work, we focused on the priming of the Quantitative Disease Resistance (QDR) in *Arabidopsis thaliana* through the application of Repeated Acoustic Stimulations (RAS). Our findings revealed a substantial increase in resistance following three consecutive stimulations, and this augmented resistance persisted consistently until 10 exposures. The observed 26% increase in resistance, irrespective of trichome presence, is intricately linked to the establishment of transcriptomic memory. This memory, characterized by dynamic interactions among a multitude of genes, facilitates the expression of numerous genes associated with disease resistance in non-inoculated plants. In the context of infection, transcriptomic memory plays a pivotal role in recruiting approximately a thousand genes potentially involved in defense, along with the extensive priming of thousands of genes. By employing a genome-scale model to elucidate gene interactions through a dynamic regulatory network, our study revealed that transcriptional memory operates in a non-hierarchical manner, engaging in the simultaneous activation of diverse biological processes associated with defense. The robustness of transcriptional memory, attributed to redundant connections between gene clusters, confers emergent properties upon primed plants. Consequently, the transcriptional memory induced by RAS displays minimal reliance on specific genes or an increased number of stimuli. However, it is worth noting that transcriptional memory is relatively short-lived and dissipates within two days after the cessation of AS.

Our results showed that the transcriptional memory of RAS triggers the expression of 102 genes associated with the MTI (Mechano-Signaling Triggered Immunity) in non-inoculated plants (Léger et al., 2022). These genes are linked to the regulation of plant defense through the mechanoperception of pathogen-derived mechanical cues through the anisotropic patterning of cortical microtubules. The repetition of mechanical stimulations enables the potentiation and acclimation of plant mechanoperception (Martin et al., 2010). The observed increase in resistance to *S. sclerotiorum* after 3 RASs may be attributed, at least in part, to the potentiation of the plant's mechanoperception, contributing to the increased effectiveness of MTI. However, the involvement of mechanosensitive-like channels (MSLs) in mechanoperception potentiation does not seem to be mediated by mechanosensitive channels or the AtMCA1 gene. This is evidenced by the restoration of the resistant phenotype in mutant lines exposed to RASs. This aligns with the biomechanics of mechanosensitive channels. AtMSL9 and AtMSL10 open at tensions on the typical magnitude of hundreds of Pascals (Peyronnet et al., 2014), which is 100 times greater than those exerted by the acoustic wave. The AtMSL10 channel can open at a frequency of 10 Hz, which is far from the 1000 Hz frequency of the acoustic wave used in this study (Tran et al., 2021). The potentiation of mechanoperception might thus be mediated by the reorganization of microtubules, in line with the enrichments of microtubule-based processes identified in clusters 4 and 22.

Epigenetic regulation plays a crucial role in the acclimation or sensitization processes of plants to repeated mechanical signals. For example, histone marks such as H3K9/14ac and H3K4me3 regulate the desensitization of poplar to repeated bending (Ghosh et al., 2023). Our data revealed that 30% of the thermal and defense memory markers are modulated by repeated acoustic stimuli (RAS). Epigenetic marks are mechanisms associated with the transcriptional memory of environmental stresses and are potentially antagonists of RNA decay (Crisp et al., 2016) which is often linked to the establishment of a new functional biological regime (Christie et al., 2011; Merret et al., 2013). Our transcriptomic data reveal that the effective establishment of priming, occurring after 3 RASs, is accompanied by robust RNA decay visible in both non-inoculated and primed plants before infection. Our simulations and experiments indicate that RAS memory persists simultaneously with RNA decay. Thus, RNA decay and epigenetic modifications may act synergistically to both maintain the memory of environmental stresses and ensure the plant's transition from a naïve state to a primed state. The transmission of epigenetic marks to offspring is one of the biological mechanisms underlying the efficacy of priming methods in agriculture. We have demonstrated that after two days, primed plants no longer exhibit a resistance gain, suggesting that RAS priming is not an effective technique for durations exceeding a few days. Similarly, the reversibility of the phenotype implies that structural modifications, such as cell wall modifications associated with RAS, are not decisive over 3 days for increasing resistance gain in primed plants.

In our approach, we employed a dynamic gene regulation model without prior assumptions at the transcriptome level. The dynamic model proved effective in predicting key emerging phenotypic characteristics associated with transcriptional memory. At the genome scale, it successfully captured the intricacies of a multi-day phenomenon, offering a temporal resolution of one day. However, its applicability in describing the actual biological regulation between genes is limited. The identified relationships among clusters primarily held mathematical significance, hindering a comprehensive understanding of the biological underpinnings governing gene interactions. This limitation notably curtailed the exploration of genes upstream of transcriptional memory, particularly those implicated in transduction processes. A potential avenue for overcoming this constraint lies in adopting a similar mathematical approach but leveraging RNA-seq data with a more refined time step, characteristic of gene interactions. This more targeted approach could reveal the early mechanisms underlying the perception of acoustic waves by plants, shedding light on the initiation of transcriptional memory. Research into the initial effects of acoustic waves (Ghosh et al., 2017) on plants suggests that a more suitable time step for such investigations would be at the minute level, representing a temporal resolution approximately 1000 times finer than the data used in the current study. Adapting to this heightened temporal resolution could unravel previously unnoticed intricacies and provide a more detailed insight into the rapid responses and regulatory mechanisms triggered by acoustic stimuli in plant systems.

An increasing number of researchers propose that it is not implausible for the acoustic component of the ecological niche to inform the plant about its environment (Appel and Cocroft, 2023; Bhandawat and Jayaswall, 2022; Demey et al., 2023; Khait et al., 2023). Apple and Cocroft (Appel and Cocroft, 2014) demonstrated that *Arabidopsis thaliana* plants exposed to vibrations caused by the chewing of *Pieris rapae* caterpillar presented higher glucosinolate levels than did plants subjected to vibrations from leafhoppers or wind. The findings of Apple and Cocroft suggest that the plant's response might be specific to the sound spectrum. In our study, the spectrum is limited to a peak at 1000 Hz. This frequency is more prominent in the spectrum of leafhoppers than in *Pieris rapae* one ((Appel and Cocroft, 2014) Fig. 4a), yet it induces effective defense. The understanding of how plants perceive acoustic waves remains a barrier preventing a satisfactory interpretation of these experimental results.

Conclusion

In this study, we investigated the effects of transcriptional memory triggered by repeated acoustic stimulations on the priming of the plant immune response. While the question of how plants perceive acoustic waves remains unanswered, the observed regulation of genes involved inMTI (Mechano-signalling Triggered Immunity) by acoustic waves suggests the potentiation of plant mechanoperception as an integral part of defense priming through acoustic stimuli. This relationship, illustrated for the first time in this work, demonstrates the potential to gain a better understanding of the molecular aspects of thigmoimmunity, i.e., the regulation of plant immunity by mechanical forces (Ghosh et al., 2021).

Utilizing RNAseq, we revealed the extent of molecular modifications associated with repeated acoustic stimulations, affecting approximately 25% of *Arabidopsis thaliana* genes. To comprehend this complexity, we inferred a dynamic genome-scale gene network. The gene network enabled us to elucidate how the robustness of genetic regulations constrains the phenotypic properties of the system. The established results, particularly the observed short duration of the transcriptional memory window, challenge the practical application of acoustic waves for crop health management in real agricultural practices. However, in this study, we opted to delineate the priming mechanisms induced by acoustic waves, which necessitate several days to manifest a phenotypic gain in resistance. Fine-tuning studies of gene expression dynamics before and after initial stimulation may help isolate a more limited number of molecular actors, providing potential new avenues for controlling breeding selection.

Material & Methods

Plant/Fungal material cultivation and inoculation

Arabidopsis plants were cultivated under constant conditions, including a 9-hour light period at 120 µmol/m²/s, a temperature of 22°C, and a relative humidity of 70% for 4 weeks before inoculation and RNA sampling. The *Sclerotinia sclerotiorum* isolate (1980) was cultured on potato dextrose agar (PDA) plates at 25°C for 3 days before inoculation. Inoculation was carried out by placing a 5 mm diameter PDA plug on the adaxial surface of *A. thaliana* leaves, following the methodology described in Barbacci et al. (2020). The mock treatment involved using an *S. sclerotiorum*-free plug. For phenotypic assessments, infections were conducted on detached leaves within a humidity-controlled chamber, facilitating disease progression imaging. RNA-seq analyses were performed on whole plants subjected to infections in the same chambers.

Phenotyping

Phenotyping was conducted on detached leaves within a controlled environment characterized by elevated humidity and a constant temperature. The enclosed space, which was equipped with a camera, captured images at 10-minute intervals. Analysis of these images allowed the measurement of lesion sizes on each leaf during infection. The susceptibility of individual leaves was subsequently calculated as the growth rate during the exponential phase of disease development, employing the segmented package in R (R Core Team, 2021). Each phenotyping analysis presented in this paper was performed independently and repeated at least three times. For more information, please consult Barbacci et al. (2020). The Python code for image analysis is available at https://github.com/darcyabjones/INFEST.

Sound priming and RNA sampling

After three weeks, the plants were transferred to two growth chambers under identical cultivation conditions. One growth chamber was equipped with a speaker (4” Visaton full range) connected to a power amplifier. The plants were subjected to acoustic stimulations during the initial three hours of the day (or the first six hours of two daily stimulations). The acoustic waves utilized were 1 kHz sinusoidal waves at a 100 dB intensity. Acoustic intensity was measured at the top of the plants via a sound intensity meter. Plants and leaves did not exhibit obvious variations in development after RAS stimulation (plant or leaf size, color, etc.). Infected plants were inoculated at the end of the final AS session. Leaf samples were collected after the last acoustic stimulation for non-inoculated plants and 24 hours post-inoculation (hpi) for infected plants. Leaves were cut with a razor blade and immediately placed on a glass cooled with liquid nitrogen as described in Sucher et al. (2020). For every plant, a 2 mm thick ring around the infected area or the *S. sclerotiorum*-free plug (mock) was taken for RNA extraction.

RNA extraction and differential gene analysis

RNA extraction was performed via the Nucleospin RNA kit from Macherey-Nagel. Subsequently, cDNA synthesis was carried out employing Superscript III reverse transcriptase (Invitrogen Carlsbad, CA) and 1 µg of total RNA. For RNA-seq, reads were concurrently mapped against the genomes of *A. thaliana* Col-0 (TAIR10 release) and *S. sclerotiorum* 1980. This was accomplished using the nf-core/rnaseq pipeline version 3.0 (Patel et al., 2020), with specific parameters, namely "--skip_alignment --pseudo_aligner salmon." This set of parameters included adapter and quality trimming using Trim Galore software version 0.6.6, followed by transcript assignment and quantification using the salmon tool (version 1.4.0).

Differential gene analysis

Three differential gene expression analyses were conducted. To elucidate the impact of repeated acoustic stimulation (RAS) on gene expression in non-inoculated plants, we utilized the gene expression levels of uninfected plants that were not exposed to acoustic stimulation as a reference. Differentially expressed genes for non-inoculated plants exposed to 1, 3, and 8 RASs were then identified through three paired statistical tests based on the negative binomial distribution. Gene expression levels associated with Bonferroni-adjusted p-values less than 0.05 were retained for further analysis. The same analytical process was employed to identify differentially expressed genes between consecutive RASs in non-inoculated plants and to understand the RASs effect on plants exposed to acoustic stimulation before infection. In the former case, the reference was the gene expression level of plants exposed to the previous RASs number. In the latter case, the reference was the gene expression level of plants not exposed to acoustic stimulation, considering infection as the reference. The analysis of differentially expressed genes was conducted via the R package DESeq2 (Love et al., 2014).

Data analysis

Enrichment analysis and graph generation were performed via ShinyGo (Ge et al., 2020). P-values are obtained via the hypergeometric test, whereas false discovery rates (FDRs) are adjusted through the Benjamini-Hochberg method to account for multiple tests. Fold enrichment is calculated as the ratio of the percentage of genes in the given list associated with a pathway to the corresponding percentage in the background gene set. While FDR is used to assess statistical significance, fold enrichment is used to quantify the effect size. Enrichments were calculated relative to a reference background. For Figures 1C and 3E, the background consisted of the set of differentially expressed genes for the previous number of AS. As shown in Figure 1C, the plants were not inoculated, whereas as shown in Figure 3E, the plants were inoculated. For the enrichments of the clusters shown in Figure 5A, enrichments were calculated relative to the set of all genes present in the 26 clusters. MTI-associated genes were extracted from Léger et al. (2022). MTI-associated genes were genes differentially expressed in the overstretched ring around the necrotic region in Col-0 compared with the impaired cortical microtubule dynamics mutant line *pfd-6*. Transcription factors and transcription factor regulations were collected from the public database PlantTFDB (Jin et al., 2017) and are available in Sfile 4. Statistics were computed using R software (R Core Team, 2021). The test used is indicated in the figure legend and the main text. Plots were made with ggplot2 (Wickham, 2009) and circlize (Gu et al., 2014) R libraries and combined with Inkscape. Graphs were plotted using Gephi free software (Bastian et al., 2009).

Clustering and dynamic gene network inference

The dataset details the expression profiles of 9954 genes that were differentially expressed across four distinct time points. The dimensions of the dataset initially posed a challenge for network inference. To address this, a crucial first step involved the substantial reduction of data dimensions using a clustering method. Traditional clustering approaches designed for static or dynamic data, such as k-means, were deemed unsuitable for our sparsely distributed temporal data. Consequently, to categorize very short time series characterized by irregularly spaced time points, we performed differential gene analysis between consecutive time measurements to elucidate the temporal variations in each gene and grouped genes with similar trajectories. Where expression significantly differed between two successive time points, the variations were designated as either positive (+) or negative (-). If the differences were not statistically significant, the temporal variation was denoted as zero (=). Subsequently, genes were organized into 27 clusters based on similar expression signatures. Notably, the cluster representing genes with a constant expression (===) was excluded from further analysis. The dynamic control network was derived through computation based on an extended explicit difference equation model, formulated as follows:

$$\Delta X_N = (X_{N+1} - X_N) = A . X_N + A S_{Systematic\,effect}$$

Here, X_N, X_{N+1}, and the $AS_{Systematic\ effect}$ are vectors of length equal to the cluster number K, and A is a K×K square matrix. This equation represents the variation in the expression of a cluster-representative gene over time as a linear combination of the expression of cluster-representative genes of all clusters and a constant term $AS_{Systematic\ effect}$. The fixed (systematic) effect of sound on cluster-representative gene expression is described by $AS_{Systematic\ effect}$. The model was constrained by the condition $A.X_0=0$, reflecting the fact that AS starts on the first day from an initial condition that we assume to be in equilibrium relative to the dynamics described by the matrix A. We also set $AS_{Systematic\ effect} = 0$ for clusters whose first transition between N=0 and N=1 was of the "=" type. To estimate A and B from the previous equation, we first imputed missing data along the trajectories at a time step of one day, using simple linear interpolation. Matrix A and vector B were estimated row by row using the Elastic net regression method, implemented in the R package glmnet (Friedman et al., 2010), with weights of 0.99 and 0.01 respectively for the lasso and ridge criteria. Lasso (Tibshirani, 1996) selected the sparsest model (largest λ values) such that MSE is within one standard error of the minimum MSE estimated with cross-validation.

Properties of Priming

To test the robustness of the gene network (**Fig. 6A**), we alternatively modified the coefficients of matrix A associated with a cluster (one line and one column) by increasing them by 1%. The effect of this variation was then evaluated by simulating the average expression trajectories of genes in each cluster (**Fig. 6A**). The RMSE of the 26 resulting trajectories was compared with the RMSE associated with the original matrix. The effect of modulating the duration between two consecutive AS events (**Fig. 6C**) was also tested through simulation by directly using Equ. 1. The eigenvalue analysis of the network was performed using the 26 eigenvalues λ_i of matrix A. The reset time of the mode p was estimated as $-1/Re(\lambda_p)$, and the period of the oscillatory mode q as $2\pi/Im(\lambda_q)$. The modes were ordered by decreasing eigenvalue modulus. As before, the contribution to gene expression of each mode was analyzed through simulation of Equ. 1.

Experimental data

SFile 1	DEG of plants exposed RASs and not inoculated
SFile 2	Evolution of GO over RAS
SFile3	MTI and thermomemory-associated genes ref
SFile4	Arabidopsis transcription factor extracted from
SFile5	DEG of plants exposed to RASs and inoculated
SFile6	Phenotypes of plants exposed to RASs

Acknowledgment

Khaoula Hadj-Amor's thesis was funded by INRAe's MathNumm department and the Occitanie region. AB and FG are funded by the templates project of the DIGITBIO metaprogram, the Thigmoimmunity project of the INRAe plant health department, and the Explorae France 2030 program SAPIENS. SR was funded by the ERC VaryWhim. The authors would like to thank Jean-Marie Frachisse and Nathalie Leblanc-Fournier for seeds

References

Aoun, N., Tauleigne, L., Lonjon, F., Deslandes, L., Vailleau, F., Roux, F., Berthomé, R., 2017. Quantitative disease resistance under elevated temperature: Genetic basis of new resistance mechanisms to ralstonia solanacearum. Front. Plant Sci. 8, 1–16. https://doi.org/10.3389/fpls.2017.01387

Appel, H., Cocroft, R., 2023. Ecology & Evolution Plant ecoacoustics : a sensory ecology approach. Trends Ecol. Evol. 1–8. https://doi.org/10.1016/j.tree.2023.02.001

Appel, H.M., Cocroft, R.B., 2014. Plants respond to leaf vibrations caused by insect herbivore chewing. Oecologia 175, 1257–1266. https://doi.org/10.1007/s00442-014-2995-6

Avramova, Z., 2019. Defence-related priming and responses to recurring drought: Two manifestations of plant transcriptional memory mediated by the ABA and JA signalling pathways. Plant Cell Environ. 42, 983–997. https://doi.org/10.1111/pce.13458

Badet, T., Léger, O., Barascud, M., Voisin, D., Sadon, P., Vincent, R., Le Ru, A., Balagué, C., Roby, D., Raffaele, S., 2019. Expression polymorphism at the ARPC4 locus links the actin cytoskeleton with quantitative disease resistance to Sclerotinia sclerotiorum in Arabidopsis thaliana. New Phytol. 222, 480–496. https://doi.org/10.1111/nph.15580

Baier, M., Bittner, A., Prescher, A., van Buer, J., 2019. Preparing plants for improved cold tolerance by priming. Plant Cell Environ. 42, 782–800. https://doi.org/10.1111/pce.13394

Barbacci, A., Lahaye, M., Magnenet, V., 2013. Another Brick in the Cell Wall: Biosynthesis Dependent Growth Model. PLoS ONE 8.

Barbacci, A., Navaud, O., Mbengue, M., Barascud, M., Godiard, L., Khafif, M., Lacaze, A., Raffaele, S., 2020. Rapid identification of an Arabidopsis NLR gene as a candidate conferring susceptibility to Sclerotinia sclerotiorum using time-resolved automated phenotyping. Plant J. 1–15. https://doi.org/10.1111/tpj.14747

Bastian, M., Heymann, S., Jacomy, M., 2009. Gephi: An Open Source Software for Exploring and Manipulating Networks. Proc. Int. AAAI Conf. Web Soc. Media 3, 361–362. https://doi.org/10.1609/icwsm.v3i1.13937

Bellec, M., Radulescu, O., Lagha, M., 2018. Remembering the past: Mitotic bookmarking in a developing embryo. Curr. Opin. Syst. Biol. 11, 41–49. https://doi.org/10.1016/j.coisb.2018.08.003

Benikhlef, L., L'Haridon, F., Abou-Mansour, E., Serrano, M., Binda, M., Costa, A., Lehmann, S., Métraux, J.-P., 2013. Perception of soft mechanical stress in Arabidopsis leaves activates disease resistance. BMC Plant Biol. 13, 133. https://doi.org/10.1186/1471-2229-13-133

Bhandawat, A., Jayaswall, K., 2022. Biological relevance of sound in plants. Environ. Exp. Bot. 200, 104919. https://doi.org/10.1016/j.envexpbot.2022.104919

Bruce, T.J.A., Matthes, M.C., Napier, J.A., Pickett, J.A., 2007. Stressful "memories" of plants: Evidence and possible mechanisms. Plant Sci. 173, 603–608. https://doi.org/10.1016/j.plantsci.2007.09.002

Cessna, S.G., Sears, V.E., Dickman, M.B., Low, P.S., 2000. Oxalic acid, a pathogenicity factor for Sclerotinia sclerotiorum, suppresses the oxidative burst of the host plant. Plant Cell 12, 2191–2199. https://doi.org/10.1105/tpc.12.11.2191

Choi, B., Ghosh, R., Gururani, M.A., Shanmugam, G., Jeon, J., Kim, J., Park, S.-C., Jeong, M.-J., Han, K.-H., Bae, D.-W., Bae, H., 2017. Positive regulatory role of sound vibration treatment in Arabidopsis thaliana against Botrytis cinerea infection. Sci. Rep. 7, 2527. https://doi.org/10.1038/s41598-017-02556-9

Christie, M., Brosnan, C.A., Rothnagel, J.A., Carroll, B.J., 2011. RNA Decay and RNA Silencing in Plants: Competition or Collaboration? Front. Plant Sci. 2. https://doi.org/10.3389/fpls.2011.00099

Conrath, U., 2011. Molecular aspects of defence priming. Trends Plant Sci. 16, 524–531. https://doi.org/10.1016/j.tplants.2011.06.004

Crisp, P.A., Ganguly, D., Eichten, S.R., Borevitz, J.O., Pogson, B.J., 2016. Reconsidering plant memory: Intersections between stress recovery, RNA turnover, and epigenetics. Sci. Adv. 2, e1501340–e1501340. https://doi.org/10.1126/sciadv.1501340

Delplace, F., Huard-Chauveau, C., Dubiella, U., Khafif, M., Alvarez, E., Langin, G., Roux, F., Peyraud, R., Roby, D., 2020. Robustness of plant quantitative disease resistance is provided by a decentralized immune network. Proc. Natl. Acad. Sci. U. S. A. 117, 18099–18109. https://doi.org/10.1073/pnas.2000078117

Demey, M.L., Mishra, R.C., Straeten, D.V.D., 2023. Sound perception in plants: from ecological significance to molecular understanding. Trends Plant Sci. 28, 825–840. https://doi.org/10.1016/j.tplants.2023.03.003

Derbyshire, M.C., Raffaele, S., 2023a. Surface frustration re-patterning underlies the structural landscape and evolvability of fungal orphan candidate effectors. Nat. Commun. 14, 5244. https://doi.org/10.1038/s41467-023-40949-9

Derbyshire, M.C., Raffaele, S., 2023b. Till death do us pair: Co-evolution of plant–necrotroph interactions. Curr. Opin. Plant Biol. 76, 102457. https://doi.org/10.1016/j.pbi.2023.102457

Desaint, H., Aoun, N., Deslandes, L., Vailleau, F., Roux, F., Berthomé, R., 2021. Fight hard or die trying: when plants face pathogens under heat stress. New Phytol. 229, 712–734. https://doi.org/10.1111/nph.16965

Didelon, M., Khafif, M., Godiard, L., Barbacci, A., Raffaele, S., 2020. Patterns of Sequence and Expression Diversification Associate Members of the PADRE Gene Family With Response to Fungal Pathogens. Front. Plant Sci. 11, 1–16. https://doi.org/10.3389/fgene.2020.00491

Engelsdorf, T., Gigli-Bisceglia, N., Veerabagu, M., McKenna, J.F., Vaahtera, L., Augstein, F., Van der Does, D., Zipfel, C., Hamann, T., 2018. The plant cell wall integrity maintenance and immune signaling systems cooperate to control stress responses in Arabidopsis thaliana. Sci. Signal. 11. https://doi.org/10.1126/scisignal.aao3070

Friedman, J.H., Hastie, T., Tibshirani, R., 2010. Regularization Paths for Generalized Linear Models via Coordinate Descent. J. Stat. Softw. 33, 1–22. https://doi.org/10.18637/jss.v033.i01

Friedrich, T., Oberkofler, V., Trindade, I., Altmann, S., Brzezinka, K., Lämke, J., Gorka, M., Kappel, C., Sokolowska, E., Skirycz, A., Graf, A., Bäurle, I., 2021. Heteromeric HSFA2/HSFA3 complexes drive transcriptional memory after heat stress in Arabidopsis. Nat. Commun. 12, 3426. https://doi.org/10.1038/s41467-021-23786-6

Ge, S.X., Jung, D., Yao, R., 2020. ShinyGO: a graphical gene-set enrichment tool for animals and plants. Bioinformatics 36, 2628–2629. https://doi.org/10.1093/bioinformatics/btz931

Ghosh, R., Barbacci, A., Leblanc-Fournier, N., 2021. Mechanostimulation: a promising alternative for sustainable agriculture practices. J. Exp. Bot. https://doi.org/10.1093/jxb/erab036

Ghosh, R., Gururani, M.A., Ponpandian, L.N., Mishra, R.C., Park, S.-C., Jeong, M.-J., Bae, H., 2017. Expression Analysis of Sound Vibration-Regulated Genes by Touch Treatment in Arabidopsis. Front. Plant Sci. 8, 100. https://doi.org/10.3389/fpls.2017.00100

Ghosh, R., Mishra, R.C., Choi, B., Kwon, Y.S., Bae, D.W., Park, S.-C., Jeong, M.-J., Bae, H., 2016. Exposure to Sound Vibrations Lead to Transcriptomic, Proteomic and Hormonal Changes in Arabidopsis. Sci. Rep. 6, 33370. https://doi.org/10.1038/srep33370

Ghosh, R., Roué, J., Franchel, J., Paul, A., Leblanc-Fournier, N., 2023. Temporal modification of H3K9/14ac and H3K4me3 histone marks mediates mechano-responsive gene expression during the accommodation process in poplar. bioRxiv 2023.02.12.526104. https://doi.org/10.1101/2023.02.12.526104

Govrin, E.M., Levine, A., 2000. The hypersensitive response facilitates plant infection by the necrotrophic pathogen Botrytis cinerea. Curr. Biol. 10, 751–757. https://doi.org/10.1016/S0960-9822(00)00560-1

Gu, Z., Gu, L., Eils, R., Schlesner, M., Brors, B., 2014. circlize implements and enhances circular visualization in R. Bioinformatics 30, 2811–2812. https://doi.org/10.1093/bioinformatics/btu393

Hassanien, R.H.E., Hou, T.Z., Li, Y.F., Li, B.M., 2014. Advances in Effects of Sound Waves on Plants. J. Integr. Agric. 13, 335–348. https://doi.org/10.1016/S2095-3119(13)60492-X

Jin, J., Tian, F., Yang, D.-C., Meng, Y.-Q., Kong, L., Luo, J., Gao, G., 2017. PlantTFDB 4.0: toward a central hub for transcription factors and regulatory interactions in plants. Nucleic Acids Res. 45, D1040–D1045. https://doi.org/10.1093/nar/gkw982

Khait, I., Lewin-Epstein, O., Sharon, R., Saban, K., Goldstein, R., Anikster, Y., Zeron, Y., Agassy, C., Nizan, S., Sharabi, G., Perelman, R., Boonman, A., Sade, N., Yovel, Y., Hadany, L., 2023. Sounds emitted by plants under stress are airborne and informative. Cell 186, 1328-1336.e10. https://doi.org/10.1016/j.cell.2023.03.009

Léger, O., Garcia, F., Khafif, M., Carrere, S., Leblanc-Fournier, N., Duclos, A., Tournat, V., Badel, E., Didelon, M., Le Ru, A., Raffaele, S., Barbacci, A., 2022. Pathogen-derived mechanical cues potentiate the spatio-temporal implementation of plant defense. BMC Biol. 20, 292. https://doi.org/10.1186/s12915-022-01495-w

Liu, H., Able, A.J., Able, J.A., 2022. Priming crops for the future: rewiring stress memory. Trends Plant Sci. 27, 699–716. https://doi.org/10.1016/j.tplants.2021.11.015

Love, M.I., Huber, W., Anders, S., 2014. Moderated estimation of fold change and dispersion for RNA-seq data with DESeq2. Genome Biol. 15, 550. https://doi.org/10.1186/s13059-014-0550-8

Martin, L., Leblanc-Fournier, N., Julien, J.L., Moulia, B., Coutand, C., 2010. Acclimation kinetics of physiological and molecular responses of plants to multiple mechanical loadings. J. Exp. Bot. 61, 2403–2412. https://doi.org/10.1093/jxb/erq069

Merret, R., Descombin, J., Juan, Y., Favory, J.-J., Carpentier, M.-C., Chaparro, C., Charng, Y., Deragon, J.-M., Bousquet-Antonelli, C., 2013. XRN4 and LARP1 Are Required for a Heat-Triggered mRNA Decay Pathway Involved in Plant Acclimation and Survival during Thermal Stress. Cell Rep. 5, 1279–1293. https://doi.org/10.1016/j.celrep.2013.11.019

Patel, H., Ewels, P., Peltzer, A., Hammarén, R., Botvinnik, O., Sturm, G., Moreno, D., Vemuri, P., Silviamorins, Pantano, L., FriederikeHanssen, Garcia, M., Rfenouil, Marchoeppner, Zhou, P., Gabernet, G., Straub, D., F., S., Bot, N., Panneerselvam, S., OMeally, D., Jun-wan, Mayer, A., Lennard, K., Tommaso, P.D., Haglund, S., Mashehu, Anil, A., Johannes Alneberg, Davenport, C., 2020. nf-core/rnaseq: nf-core/rnaseq v3.0 - Silver Shark. https://doi.org/10.5281/zenodo.4323183

Peyronnet, R., Tran, D., Girault, T., Frachisse, J.-M., 2014. Mechanosensitive channels: feeling tension in a world under pressure. Front. Plant Sci. 5, 558. https://doi.org/10.3389/fpls.2014.00558

Poland, J.A., Balint-Kurti, P.J., Wisser, R.J., Pratt, R.C., Nelson, R.J., 2009. Shades of gray: the world of quantitative disease resistance. Trends Plant Sci. 14, 21–29. https://doi.org/10.1016/j.tplants.2008.10.006

Proseus, T.E., Boyer, J.S., 2006. Calcium pectate chemistry controls growth rate of Chara corallina. J. Exp. Bot. 57, 3989–4002. https://doi.org/10.1093/jxb/erl166

R Core Team, 2021. R: A Language and Environment for Statistical Computing.

Raffaele, S., Farrer, R.A., Cano, L.M., Studholme, D.J., MacLean, D., Thines, M., Jiang, R.H.Y., Zody, M.C., Kunjeti, S.G., Donofrio, N.M., Meyers, B.C., Nusbaum, C., Kamoun, S., 2010. Genome evolution following host jumps in the irish potato famine pathogen lineage. Science 330, 1540–1543. https://doi.org/10.1126/science.1193070

Remick, B.C., Gaidt, M.M., Vance, R.E., 2023. Effector-Triggered Immunity. Annu. Rev. Immunol. 41, 453–481. https://doi.org/10.1146/annurev-immunol-101721-031732

Roux, F., Voisin, D., Badet, T., Balagu??, C., Barlet, X., Huard-Chauveau, C., Roby, D., Raffaele, S., 2014. Resistance to phytopathogens e tutti quanti: Placing plant quantitative disease resistance on the map. Mol. Plant Pathol. 15, 427–432. https://doi.org/10.1111/mpp.12138

Ru, C., Hu, X., Chen, D., Wang, W., 2024. Drought stimulus enhanced stress tolerance in winter wheat (*Triticum aestivum* L.) by improving physiological characteristics, growth, and water productivity. Plant Physiol. Biochem. 214, 108906. https://doi.org/10.1016/j.plaphy.2024.108906

Singh, B.K., Delgado-Baquerizo, M., Egidi, E., Guirado, E., Leach, J.E., Liu, H., Trivedi, P., 2023. Climate change impacts on plant pathogens, food security and paths forward. Nat. Rev. Microbiol. 21, 640–656. https://doi.org/10.1038/s41579-023-00900-7

Sucher, J., Mbengue, M., Dresen, A., Barascud, M., Didelon, M., Barbacci, A., Raffaele, S., 2020. Phylotranscriptomics of the Pentapetalae Reveals Frequent Regulatory Variation in Plant Local Responses to the Fungal Pathogen Sclerotinia sclerotiorum. Plant Cell tpc.00806.2019. https://doi.org/10.1105/tpc.19.00806

Thellier, M., Lüttge, U., Norris, V., Ripoll, C., 2018. Plant Accommodation to Their Environment: The Role of Specific Forms of Memory, in: Baluska, F., Gagliano, M., Witzany, G. (Eds.), Memory and Learning in Plants. Springer International Publishing, Cham, pp. 131–137. https://doi.org/10.1007/978-3-319-75596-0_7

Tibshirani, R., 1996. Regression Shrinkage and Selection Via the Lasso. J. R. Stat. Soc. Ser. B Methodol. 58, 267–288. https://doi.org/10.1111/j.2517-6161.1996.tb02080.x

Tran, D., Girault, T., Guichard, M., Thomine, S., Leblanc-Fournier, N., Moulia, B., de Langre, E., Allain, J.M., Frachisse, J.M., 2021. Cellular transduction of mechanical oscillations in plants by the plasma-membrane mechanosensitive channel MSL10. Proc. Natl. Acad. Sci. U. S. A. 118. https://doi.org/10.1073/PNAS.1919402118

Verhagen, B.W.M., Trotel-Aziz, P., Couderchet, M., H??fte, M., Aziz, A., 2010. Pseudomonas spp.-induced systemic resistance to Botrytis cinerea is associated with induction and priming of defence responses in grapevine. J. Exp. Bot. 61, 249–260. https://doi.org/10.1093/jxb/erp295

Wang, X., Vignjevic, M., Jiang, D., Jacobsen, S., Wollenweber, B., 2014. Improved tolerance to drought stress after anthesis due to priming before anthesis in wheat (Triticum aestivum L.) var. Vinjett. J. Exp. Bot. 65, 6441–6456. https://doi.org/10.1093/jxb/eru362

Wang, Z., Ma, L.-Y., Cao, J., Li, Y.-L., Ding, L.-N., Zhu, K.-M., Yang, Y.-H., Tan, X.-L., 2019. Recent Advances in Mechanisms of Plant Defense to Sclerotinia sclerotiorum. Front. Plant Sci. 10, 1314. https://doi.org/10.3389/fpls.2019.01314

Wickham, H., 2009. Ggplot2 9–27. https://doi.org/10.1007/978-0-387-98141-3

Yamanaka, T., Nakagawa, Y., Mori, K., Nakano, M., Imamura, T., Kataoka, H., Terashima, A., Iida, K., Kojima, I., Katagiri, T., Shinozaki, K., Iida, H., 2010. MCA1 and MCA2 that mediate Ca2+ uptake have distinct and overlapping roles in Arabidopsis. Plant Physiol. 152, 1284–1296.

https://doi.org/10.1104/pp.109.147371